Journal of Alloys and Compounds 509 (2011) 5617–5622

Contents lists available at ScienceDirect

Journal of Alloys and Compounds

journal homepage: www.elsevier.com/locate/jallcom

Hydrothermal synthesis of PtRu on CNT/SnO_2 composite as anode catalyst for methanol oxidation fuel cell

Nitul Kakati, Jatindranath Maiti, Seung Hyun Jee, Seok Hee Lee, Young Soo Yoon*

Department of Materials Science and Engineering, Yonsei University, 134 Shinchon-dong, Seodaemun-gu, Seoul, 120-749, Republic of Korea

ARTICLE INFO

Article history:
Received 16 November 2010
Received in revised form 15 February 2011
Accepted 16 February 2011
Available online 23 February 2011

Keywords:
Fuel cell
CNT/SnO_2 composite
PtRu alloy
Methanol oxidation

ABSTRACT

An electrocatalyst support comprising of carbon nanotube and tin oxide (CNT/SnO_2) was prepared by an ethylene glycol mediated synthesis procedure and proposed as an improved catalyst support for direct methanol fuel cell. CNTs are covered by the porous SnO_2 layer which is homogeneously distributed over CNT surface. PtRu alloy nanoparticles were deposited over this composite material by a hydrothermal synthesis method. The CNT/SnO_2 composite and its supported PtRu catalyst (PtRu/SnO_2/CNT) were characterized by X-ray diffraction, field emission scanning electron microscopy and transmission electron microscopy. The electrocatalytic activity of PtRu/SnO_2/CNT catalyst for methanol oxidation has been studied by cyclic voltammetry, impedance spectroscopy and chronoamperometry. The results were compared with Pt/SnO_2/CNT and PtRu/CNT catalysts synthesized by the same procedure. PtRu/SnO_2/CNT catalyst shows an electrochemically active surface area of 81.84 $m^2\,g_{Pt}^{-1}$ and a mass activity of 890 $mA\,mg_{Pt}^{-1}$. The presence of SnO_2 layer over CNT can further improve the electrocatalytic activity of PtRu alloy nanoparticles for methanol oxidation.

1. Introduction

Recently, electro-oxidation of small organic molecules has attracted much attention due to the development of direct liquid fuel cells with their high energy density [1]. Therefore a much afford has been offered on the development of electrocatalyst for the direct methanol fuel cell (DMFC) in the last two decades [2,3]. Now, one of the main goals in DMFC research is to develop electrocatalyst having high activity and anti-poisoning ability. It is well known that the main problem with platinum, the best single metal catalyst for methanol oxidation is poisoning of its active sites by the intermediates such as CO_{ads} [4,5]. Up to the present, Ru has been regarded as best supporting metal for Pt to remove CO_{ads} and accelerate methanol oxidation [6–8]. Recently a trend in catalyst research of fuel cells is emerging out of the advantages of metal oxides in relaxing CO_{ads} on Pt surface. Lee et al. found that $RuSnO_2$ supported Pt catalysts showed higher oxidation current in comparison with Pt/VulcanXC-72 [9]. Ahn et al. suggested Pt–CeO_2 nanocomposite thin films prepared by co-sputtering method under optimum conditions which may serve as a potentially important tool for the fabrication of high performance direct methanol thin film fuel cells [10]. Villullus et al. prepared a Pt–RuO_2/Ti electrode by a sol–gel method which exhibited an enhancement effect for the oxidation of methanol that can be interpreted as associated to the formation of hydrous oxides on the RuO_2 surface [11]. Several papers reported a higher current density of methanol and ethanol oxidation using SnO_2 with Pt catalyst than the pure Pt catalyst [12,13]. Matsui et al. reported electrochemical oxidation of CO over tin oxide supported platinum catalyst and found an enhancement of CO tolerance over Pt/SnO_x compared to Pt/C [14]. Saha et al. prepared a composite electrode by electrochemical deposition of PtRu onto the surface of SnO_2 nanowires directly grown on the carbon paper. They found a higher oxidation performance than the commercial electrocatalyst for methanol oxidation [15]. Low durability has been recognized as one of the most important issues of the proton exchange membrane fuel cells including DMFC [16,17]. It has been found that presence of SnO_2 provide the catalyst material a high durability [18]. It is because of stability of SnO_2 which is very high in dilute acidic solution. It has been reported that the presence of SnO_2 in the vicinity of Pt catalyst could supply oxygen-containing species for the oxidative removal of CO_{ads} species from the Pt surface during methanol oxidation [19]. The adsorption and decomposition of methanol occur at Pt sites while the decomposition of water occurs over SnO_2 sites to form oxygen-containing species which can react with CO_{ads} species produced during methanol oxidation. However, as a catalyst support, the conductance of SnO_2 still needs to be improved. To be used as catalyst support, the materials should have proper physical properties such as high electron conductivity, surface functional groups, high mechanical strength, high surface area, a proper pore size, and a proper shape. To enhance the electronic

* Corresponding author. Tel.: +82 2 2123 2847; fax: +82 2 365 5882.
E-mail address: yoonys@yonsei.ac.kr (Y.S. Yoon).

0925-8388/$ – see front matter © 2011 Elsevier B.V. All rights reserved.
doi:10.1016/j.jallcom.2011.02.087

property, SnO_2 can be used with CNT to form composite material to apply as a catalyst support. However, the conductivity of this composite material can be further improved when the SnO_2 particles are deposited homogeneously over the surface of the CNT. Recently Wang et al. reported a SnO_2/graphene hybrid nanocomposite by a microwave polyol synthesis which is more efficient than graphene for supercapacitor [20]. Du et al. [18] proposed a mesoporous SnO_2 coated CNTs core sheath nanocomposite prepared by hydrothermal method as a catalyst support for proton exchange membrane fuel cells (PEMFCs). They found that this catalyst support was more corrosion resistant than CNT support. Also due to the formation of mesopores by SnO_2 particles can prevent the migration of Pt nanoparticles thereby preventing aggregation. However, Ru is more effective than SnO_2 in promoting CO_{ads} electro-oxidation at relatively higher potential [21,22]. Therefore we use both Ru and SnO_2 with platinum to minimize the poisoning effect of CO_{ads} on platinum active sites.

It has been found that tin oxide material is difficult to deposit uninterruptedly over the CNT surface by a solution route; therefore it becomes difficult to completely exploit the benefit of this material. In this article we have reported an ethylene glycol (EG) and polyvinyl pyrrolidone (PVP) assisted simple and efficient solution based synthesis method for the CNT/SnO_2 composite. We have deposited Pt–Ru alloy nanoparticles on the surface of synthesized composite material by hydrothermal process. Hydrothermal condition can provide a uniform environment for the nucleation and growth of metal particles. The electrocatalytic activity of the material has been reported here.

2. Experimental

2.1. Synthesis of CNT/SnO_2 composite

0.05 g $SnC_2O_4{\cdot}2H_2O$ (partially dissolved in 3 ml EG), 0.25 g PVP (dissolved in 3 ml EG) and 0.1 g MWCNTs were added to the solution mixture with 10 ml of EG. Prior to use, raw MWCNTs were treated with 70% nitric acid at 120 °C for 4 h to increase their hydrophilicity. The solution mixture was then hosted in a round bottom flask and refluxed at 195 °C under the ambient pressure. The solution had been refluxed under constant stirring for two and half hour and then the reaction was stopped. After cooling down the solution to room temperature the precipitates were collected by centrifugation at 8000 rpm followed by washing with ethanol and water to remove physically adsorbed PVP and EG. The precipitates were then dried at 80 °C in an oven. After that the composite was annealed for 1 h at 300 °C. For the deposition of PtRu nanoparticles the surface activation of the composite material is necessary. Therefore we have treated the composite material with 5 M HNO_3 for 6 h. Then the composite material was again dried at 80 °C in an oven for overnight. Now the material is ready for use as a catalyst support.

2.2. Preparation of electrocatalysts and characterization of materials

PtRu/SnO_2/CNT was prepared by using $H_2PtCl_6{\cdot}6H_2O$ and $RuCl_3$ as the metal source and using ethylene glycol (EG) as reducing agent under hydrothermal condition. Briefly the preparation procedure consisted of the following steps: 2.0 ml 0.05 M $H_2PtCl_6{\cdot}6H_2O$ and 2.0 ml 0.05 M $RuCl_3$ aqueous solution was mixed with 30 ml of EG. The atomic composition of Pt and Ru was 1:1. To adjust the pH value, 0.4 M KOH was added dropwise under magnetic stirring until it reaches to 8. About 70 mg of pretreated CNT/SnO_2 were added into the solution, and the solution was sonicated for 1 h. After 3 h of magnetic stirring the solution was transferred into an autoclave container and sealed to perform hydrothermal treatment at 150 °C for 5 h. The resulting suspension was filtered and washed with copious distilled water and ethanol respectively. The resulting catalyst paste was finally dried at 80 °C in a vacuum oven for overnight.

To compare the electrocatalytic performance of PtRu/SnO_2/CNT, PtRu/CNT (Pt:Ru = 1:1) and Pt/SnO_2/CNT were also prepared using the same method.

X-ray diffraction (XRD) analysis was carried out on a Rigaku X-ray diffractometer with Cu Kα radiation (λ = 1.5418 Å). The morphology and dispersion of the samples were observed on a TEM (JEM-4010, JEOL) equipped with an EDS detector. FESEM and energy dispersive spectroscopy (EDS) for quantitative analysis of the samples were carried out with a (FESEM JSM-6700F, JEOL) coupled with INCA energy dispersive X-ray spectroscopy.

Table 1
EDS Results of as synthesized catalysts.

Sample	Pt:Ru atomic (%)	
	Nominal content	Actual content
Pt/SnO_2/CNT	50:0	50:0
PtRu/SnO_2/CNT	50:50	50.1:49.9
PtRu/CNT	50:50	55:45

2.3. Electrochemical analysis for the catalysts

Cyclic voltammetry, chronoamperometry and impedance measurement were carried out on electrochemical workstation IM6e (Zahner) in a three-electrode test cell at room temperature. The impedance spectra were recorded between 100 kHz and 100 mHz. The working electrode was a glassy carbon electrode having a diameter of 3 mm. 5 mg of the sample was dissolved in 2 ml of 0.05% nafion solution and then sonicated for 30 min. After that 5 μl of the slurry was injected and spread on the glassy carbon electrode. The electrode was then dried at 80 °C. At this amount of slurry the catalyst loading was about 0.178 mg cm^{-2} based on this geometric area. A saturated calomel electrode (SCE) and a Pt wire were used as the reference and counter electrodes respectively. All electrolytes were deaerated by bubbling pure N_2 for 20 min and protected with a nitrogen atmosphere during the entire experimental procedure.

3. Results and discussion

Fig. 1 presents the FESEM images showing the structure of the CNT/SnO_2 and PtRu/SnO_2/CNT. It can be clearly observed that CNTs are homogeneously covered by the SnO_2 layer with a porous morphology. To facilitate electron transport during the electrochemical reactions, a porous structure of the support is suitable for maximum contact with fuel or oxidant and strong interaction between the catalyst and the support [9]. The key step of formation of a homogeneous and porous SnO_2 layer can be described on the basis of oligomerization of tin glycolates [23]. At the initial stage of refluxing, the oxalate groups of SnC_2O_4 were replaced gradually by ethylene glycol units through the formation of Sn–O– covalent and Sn←OH coordination bonds and subsequently deposited onto the CNT surface. As refluxing was continued tin glycolates underwent several steps of intermediate reactions and eventually formation of uninterrupted grains and further self assembled to cover the surface of CNTs. From the morphology of the composite material it can be confirmed that SnO_2 layer can protect the CNT surface from the electrochemical corrosion and prevents Pt–Ru nanoparticles agglomeration. The process of formation of catalyst structure is shown in Scheme 1.

From the TEM image of a single CNT covered with PtRu/SnO_2, we can observe that the particles are dispersed uniformly on the surface of the CNT. Although it is difficult for us to distinguish between PtRu and SnO_2 particles in Fig. 2a we have calculated the particle size from the XRD results by using Scherrer formula. In Fig. 2b, EDS line spectra clearly show the structural information of the catalyst. It has been observed from the EDS line spectra that the PtRu alloy nanoparticles are deposited homogeneously on the CNT/SnO_2 composite. The results of the EDS analysis are given in Table 1 which shows the nominal content and actual content of the catalysts.

Fig. 3 shows the XRD patterns of the CNT/SnO_2 nanocomposite, Pt/SnO_2/CNT, PtRu/SnO_2/CNT and PtRu/CNT electrocatalysts. For CNT, generally the peak associated with the (0 0 2) diffraction is located at about 26.0°. Here the SnO_2 (1 1 0) and CNT (0 0 2) peaks are completely overlapped with one another. Further the (1 0 1), (2 1 1) peaks for SnO_2 were broad and indicates a small size of the SnO_2 nanoparticles. The average particle size of the SnO_2 was calculated from Scherrer formula and found 5.3 nm. For Pt and PtRu the (1 1 1), (2 0 0), (2 2 0) and (3 1 1) peaks were observed. The average particle size of PtRu in PtRu/SnO_2/CNT and PtRu/CNT were 2.5 and 3.1 nm respectively and for Pt nanoparticles in Pt/SnO_2/CNT

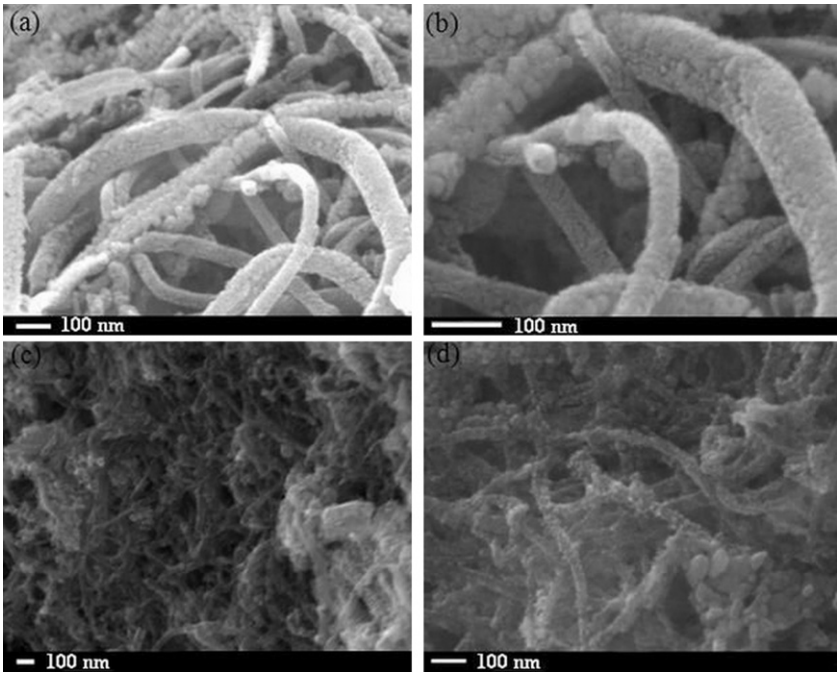

Fig. 1. FESEM images of (a) and (b) CNT/SnO_2 composite and (c) and (d) PtRu/SnO_2/CNT catalyst.

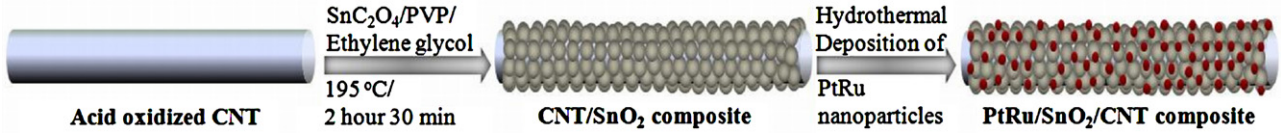

Scheme 1. Schematic diagram of the formation of catalyst supported on CNT/SnO_2 composite.

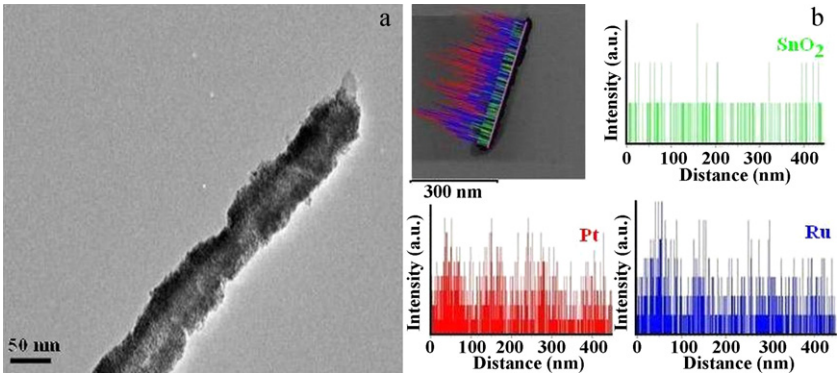

Fig. 2. (a)TEM image of PtRu/SnO_2/CNT catalyst and (b) EDS line spectra of PtRu/SnO_2/CNT catalyst.

was 3.5 nm. In case of PtRu alloy nanoparticles Pt fcc structure slightly shifted to higher 2θ which corresponds to a decrease in lattice constant compared to pure platinum fcc structure due to the incorporation of Ru atoms [24].

The Pt or PtRu decorated CNT/SnO_2 composite was further evidenced by a series of electrochemical experiments. In Fig. 4 the hydrogen absorption peaks appeared in the potential range between 0.08 and 0.13 V. The potential of hydrogen absorption peak for PtRu/CNT was found little higher than the catalysts prepared using CNT/SnO_2 composite. This potential difference reveals the presence of a strong interaction between catalyst particles with SnO_2 particles [25]. The electrochemically active surface area (S_{EAS}) is calculated from the following equation based on hydrogen adsorption–desorption (area with oblique lines in Fig. 4) voltametry.

$$S_{EAS} = \frac{Q_1}{G \times Q_2} \quad (1)$$

where Q_1 is the charge quantity consumed from integrated in CV curves for hydrogen adsorption–desorption in micro-Coulomb (μC), G represents the total metal loading (μg) in electrode, Q_2 is the charge required to oxidize a single layer saturation coverage hydrogen on Pt surface area of 210 ($\mu C\,cm^{-2}$) [26]. The calculated value of S_{EAS} for Pt/SnO_2/CNT is 205.90 $m^2\,g^{-1}$, while that for PtRu/SnO_2/CNT and PtRu/CNT are 81.84 $m^2\,g^{-1}$ and 134 $m^2\,g^{-1}$. The active sites of Pt decreases due to alloy formation with ruthenium in case of PtRu/SnO_2/CNT and PtRu/CNT catalysts. In case of PtRu/SnO_2/CNT platinum active sites may be further blocked by the

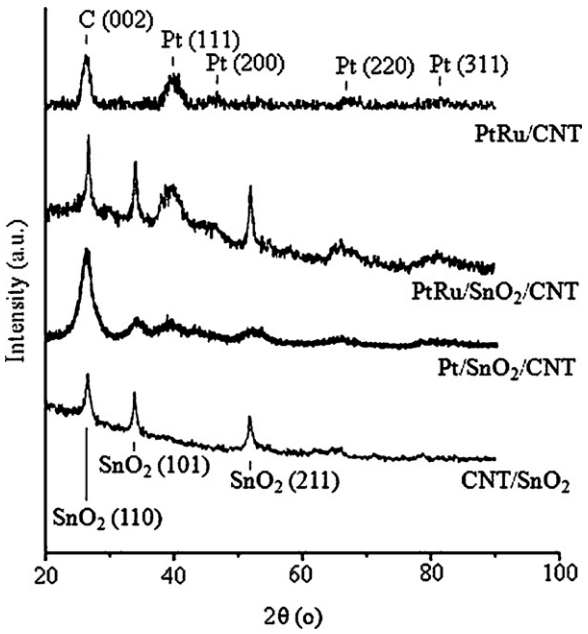

Fig. 3. XRD patterns of the composites.

SnO_2 particles. However these S_{EAS} values look abnormally higher as compared to SnO_2 modified PtRu/C catalyst prepared by Wang et al. despite of having a smaller particle size calculated from XRD [27]. A high value of S_{EAS} for all the catalysts can be attributed to the porous structure of the catalyst support. These values were also found higher than the catalysts synthesized by Saha et al. [12,15] using SnO_2 nanowire on carbon paper. It is worth mentioning that using CNT as the support for SnO_2 particles provides higher surface area with improved electrical properties than using carbon black and SnO_2 particles as support material.

Fig. 5 compares the CV currents for PtRu/SnO_2/CNT with PtRu/CNT and Pt/SnO_2/CNT electrocatalysts. All electrochemical experiments were done in solution mixture containing 1 M methanol and 0.5 M H_2SO_4 solution. As seen from Fig. 5 the PtRu/SnO_2/CNT catalyst had a higher current density of about 57 mA cm^{-2} at 0.80 V than the PtRu/CNT (49 mA cm^{-2} at 0.80 V) and Pt/SnO_2/CNT (10 mA cm^{-2} at 0.92 V) catalysts. The PtRu/SnO_2/CNT electrocatalyst showed a lower onset potential (0.33 V) than the PtRu/CNT catalyst (0.37 V) and Pt/SnO_2/CNT catalyst (0.45 V). The forward peak current density (I_f) is generally regarded as methanol oxidation on non-poisoned catalysts, while the backward peak current density (I_b) is associated with methanol oxidation on regenerated catalysts (after the removal of the carbonaceous intermediate) [28]. The I_f to I_b ratio, is an index of the catalyst tolerance to the poisoning species. A higher ratio indicates more effective removal of the poisoning species on the catalyst surface. The ratio is found almost ten times higher for the PtRu/SnO_2/CNT than the PtRu/CNT and thirty times higher than Pt/SnO_2/CNT. Mass activity (MA) of the catalysts has been introduced and defined as follows [29]:

$$MA = \frac{i_p}{m_d} \times 10^3 \quad (2)$$

Here i_p (mA cm^{-2}) is the peak current density obtained from forward oxidation peak, and m_d (μg cm^{-2}) is the loading mass of Pt. The loading mass of Pt can be calculated based on the mass of H_2PtCl_6. The MA has significant implications for fuel cells, because the cost of electrode largely depends on the total catalyst used. From Fig. 5 the maximum MA value of the PtRu/SnO_2/CNT catalyst can be obtained and it is 890 mA mg^{-1}, which is higher than

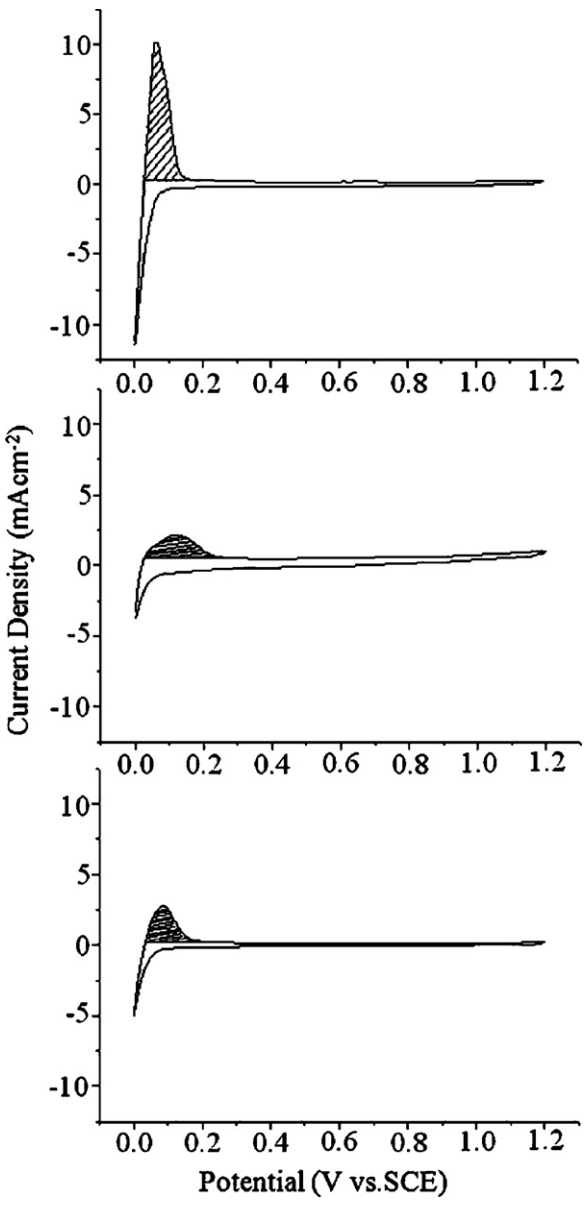

Fig. 4. Cyclic voltametry curves of (a) Pt/SnO_2/CNT (b) PtRu/SnO_2/CNT and (c) PtRu/CNT in N_2 saturated solution of 0.5 mol L^{-1} H_2SO_4 at room temperature and a scan rate of 20 mV s^{-1}.

PtRu/CNT (769 mA mg^{-1}) catalyst and Pt/SnO_2/CNT (134 mA mg^{-1}) catalyst prepared by the same method. Such a high value of mass activity may be achieved due to homogeneous and porous SnO_2 layer over CNT which enhances the electronic properties of the catalyst support. Also hydrothermal synthesis provides homogeneous dispersion of catalyst particles.

The high durability of the power sources is one of the main requirements for practical applications. The long term stability of the electrocatalysts was observed by plotting current–time (i–t) curves in Fig. 6 at a fixed potential of 0.60 V. PtRu/SnO_2/CNT has a higher current at all time than PtRu/CNT electrocatalyst and Pt/SnO_2/CNT. The decay ratio (ratio of maximum current to minimum current in Fig. 6) of current density on the PtRu/SnO_2/CNT (1.33) is also found less than PtRu/CNT (1.83) and Pt/SnO_2/CNT (5.55) which implies enhanced electrocatalytic activity and better tolerance to poisoning species of PtRu/SnO_2/CNT catalyst. The impedance patterns of the Pt/SnO_2/CNT, PtRu/SnO_2/CNT and PtRu/CNT electrocatalysts in an N_2 saturated solution of 0.5 mol L^{-1}

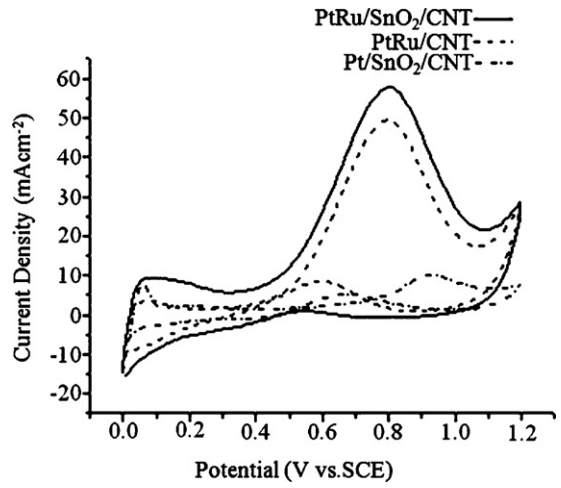

Fig. 5. Cyclic voltametry curves of the catalysts in N_2 saturated solution of 1 mol L^{-1} CH_3OH and 0.5 mol L^{-1} H_2SO_4 at room temperature and a scan rate of 20 mV s^{-1}.

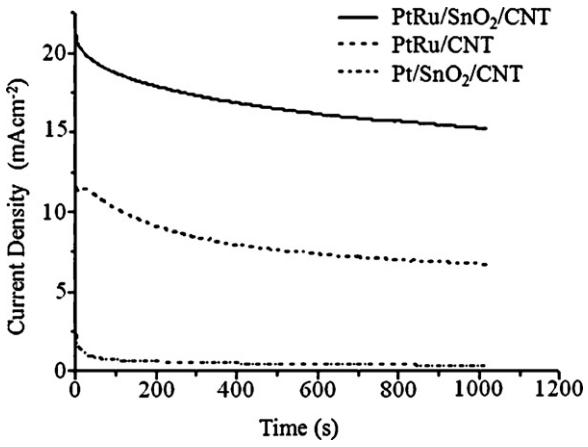

Fig. 6. Chronoamperometry curves of the catalysts in N_2 saturated solution of 1 mol L^{-1} CH_3OH and 0.5 mol L^{-1} H_2SO_4 at room temperature and a fixed potential of 0.6 V.

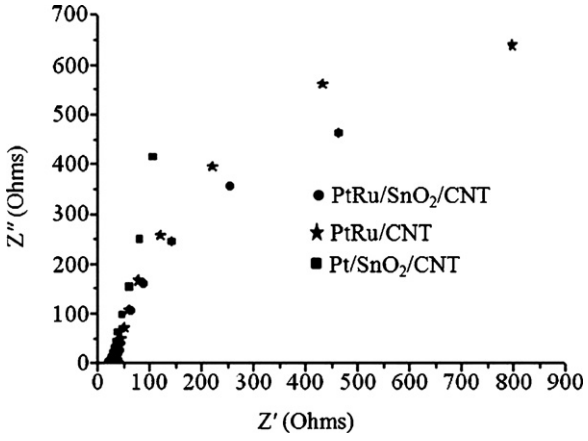

Fig. 7. Impedance spectra of the catalysts in N_2 saturated solution of 1 mol L^{-1} CH_3OH and 0.5 mol L^{-1} H_2SO_4 at room temperature and a fixed potential of 0.5 V.

H_2SO_4 and 1.0 mol L^{-1} CH_3OH at 25 °C at 0.5 V are shown in Fig. 7. The Faradaic admittance of methanol electrooxidation is [30]:

$$\gamma_F = \frac{1}{R_{ct}} + \frac{B}{a + j\omega} \quad (3)$$

Table 2
Electrochemical Properties of as synthesized catalysts.

Sample	S_{EAS} (m^2 g_{Pt}^{-1})	MA (mA mg_{Pt}^{-1})	I_f/I_b	Decay ratio
$Pt/SnO_2/CNT$	205.90	134	1.85	5.55
$PtRu/SnO_2/CNT$	81.84	890	56.4	1.33
PtRu/CNT	134	769	5.76	1.83

where $R_{ct} = (\delta E/\delta I_F)_{ss}$ is the charge transfer resistance at steady state of the electrode reaction. Its value is always positive. I_F is the Faraday current. It can be seen from figure that the (R_{ct}) for methanol electrooxidation on $PtRu/SnO_2/CNT$ is lower than that of the PtRu/CNT and $Pt/SnO_2/CNT$. Thus the performance of the CO tolerance on the $PtRu/SnO_2/CNT$ catalyst is higher than that on the other two catalysts.

It is observed from all the electrochemical results (Table 2) that the presence of SnO_2 can further improve the electrocatalytic activity of the catalyst for methanol oxidation when used with Pt and Ru. $PtRu/SnO_2/CNT$ exhibits better electrochemical activity towards methanol oxidation than the other two catalysts although it shows lower S_{EAS} value. Sn sites predominantly adsorb OH_{ads} and H_2O_{ads} [31]. The removal of CO_{ads} on Pt and Ru sites proceeded via its reaction with OH_{ads} on Sn sites. Once the CO_{ads} on Ru sites were electro-oxidized, OH_{ads} were produced on Ru sites at a faster rate than SnO_2 sites. During the methanol electro-oxidation, CO_{ads} also could migrate from Pt sites to Ru sites [27], and therefore addition of SnO_2 with PtRu provides an additional route for OH_{ads} formation and hence accelerates methanol oxidation.

4. Conclusions

CNT/SnO_2 composite was prepared by an ethylene glycol (EG) assisted simple and efficient solution based synthesis method. Pt or PtRu alloy catalyst particles were deposited by a hydrothermal process. SnO_2 particles were homogenously distributed over the CNT surface. We have found that presence of SnO_2 along with Ru further enhances the catalytic activity of Pt for methanol oxidation. Although the electrochemically active surface area for $PtRu/SnO_2/CNT$ was found lower than $Pt/SnO_2/CNT$ and PtRu/CNT, it shows greater activity for methanol oxidation at room temperature. The catalysts showed a very high mass activity for methanol oxidation. The high catalytic activity of the catalyst can be attributed to homogeneous and porous SnO_2 layer over CNT which enhances the catalyst and fuel interaction.

Acknowledgements

This work was supported by Priority Research Centers Program through the National Research Foundation of Korea (NRF) funded by the Ministry of Education, Science and technology (2009-0093823) and financially supported by a grant to MEMS Research Center for National defense funded by Defense Acquisition Program. We are also thankful to Defense Nano Technology (Center), Korea for supporting this research.

References

[1] W. Vielstich, J. Braz. Chem. Soc. 14 (2003) 503–509.
[2] E. Antolini, J.R.C. Salgado, E.R. Gonzalez, J. Electroanal. Chem. 580 (2005) 145–154.
[3] Y.M. Alyousef, M.K. Datta, K. Kadakia, S.C. Yao, P.N. Kumta, J. Alloys Compd. 506 (2010) 698–702.
[4] U.A. Paulus, U. Endruschat, G.J. Feldmeyer, T.J. Schmidt, H. Bonnemann, R.J. Behm, J. Catal. 195 (2000) 383–393.
[5] E. Antolini, Mater. Chem. Phys. 78 (2003) 563–573.
[6] Y.J. Song, S.B. Han, J.M. Lee, K.W. Park, J. Alloys Compd. 473 (2009) 516–520.
[7] J.M. Sieben, M.M.E. Duarte, C.E. Mayer, J. Alloys Compd. 509 (2011) 4002–4009.
[8] Y.C. Wei, C.W. Liu, W.J. Chang, K.W. Wang, J. Alloys Compd. 509 (2011) 535–541.

[9] J.M. Lee, S.B. Han, Y.W. Lee, Y.J. Song, J.Y. Kim, K.W. Park, J. Alloys Compd. 506 (2010) 57–62.
[10] H.J. Ahn, J.S. Jang, Y.E. Sung, T.Y. Seong, J. Alloys Compd. 473 (2009) L28–L32.
[11] H.M. Villullus, F.I. Mattos-Costa, L.O.S. Bulhoes, J. Phys. Chem. B 108 (2004) 12898–12903.
[12] M.S. Saha, R. Li, M. Cai, X. Sun, Electrochem. Solid-State Lett. 10 (8) (2007) B130–B133.
[13] H.L. Pang, J.P. Lu, J.H. Chen, C.T. Huang, B. Liu, X.H. Zhang, Electrochim. Acta 54 (2009) 2610–2615.
[14] T. Matsui, K. Fujiwara, T. Okanishi, R. Kikuchi, T. Takeguchi, K. Eguchi, J. Power Sources 155 (2006) 152–156.
[15] M.S. Saha, R. Li, X. Sun, Electrochem. Commun. 9 (2007) 2229–2234.
[16] J. Xie, D.L. Wood, D.M. Wayne, T.A. Zawodzinski, P. Atnassov, R.L. Borup, J. Electrochem. Soc. 152 (2005) A104–A113.
[17] S. Takenaka, H. Matsumori, K. Nakagawa, H. Matsune, E. Tanabe, M. Kishida, J. Phys. Chem. C 111 (2007) 15133–15136.
[18] C. Du, M. Chen, X. Cao, G. Yin, P. Shi, Electrochem. Commun. 11 (2009) 496–498.
[19] E. Antolini, F. Colmati, E.R. Gonzalez, Electrochem. Commun. 9 (2007) 398–404.
[20] S. Wang, S.P. Jiang, X. Wang, Electrochim. Acta (2011), doi:10.1016/j.electacta.2011.01.016.
[21] L Jiang, L. Colmenares, Z. Jusys, G.Q. Sun, R.J. Behm, Electrochim. Acta 53 (2007) 377–389.
[22] Q. Wang, G.Q. Sun, L.H. Jiang, Q. Xin, S.G. Sun, Y.X. Jiang, S.P. Chen, Z. Jusys, R.J. Behm, Phys. Chem. Chem. Phys. 9 (2007) 2686–2696.
[23] Y. Wang, X. Jiang, Y. Xia, J. Am. Chem. Soc. 125 (2003) 16176–16177.
[24] E. Antolini, F. Cardellini, J. Alloys Compd. 315 (2001) 118–122.
[25] N. Shang, P. Papakonstantinou, P. Wang, S.R.P. Silva, J. Phys. Chem. C 114 (2010) 15837–15841.
[26] Z.B. Wang, P.J. Zuo, G.P. Yin, Fuel Cells 9 (2009) 106–113.
[27] G. Wang, T. Takeguchi, Y. Zhang, E.N. Muhamad, M. Sadakane, S. Ye, W. Ueda, J. Electrochem. Soc. 156 (2009) B862–B869.
[28] J. Prabhuram, R. Manoharan, J. Power Sources 74 (1998) 54.
[29] H. Tang, J.H. Chen, L.H. Nie, D.Y. Liu, W. Deng, Y.F. Kuang, S.Z. Yao, J. Colloid Interface Sci. 269 (2004) 26–31.
[30] G. Wu, L. Li, B.Q. Xu, Electrochim. Acta 50 (2004) 1–10.
[31] K. Wang, H.A. Gasteiger, N.M. Markovic, P.N. Ross, Elecctrochim. Acta 41 (1996) 2587–2593.